




# Direct evidence of a charge depletion region at the interface of van der Waals monolayers and dielectric oxides: The case of superconducting FeSe/STO

Khalil Zakeri <sup>1,\*</sup>, Dominik Rau,<sup>1</sup> Janek Wettstein <sup>1</sup>, Markus Döttling <sup>1</sup>, Jasmin Jandke,<sup>2</sup>  
Fang Yang,<sup>2</sup> Wulf Wulfhekel,<sup>2,3</sup> and Jörg Schmalian<sup>4,3</sup>

<sup>1</sup>Heisenberg Spin-Dynamics Group, Physikalisches Institut, Karlsruhe Institute of Technology,  
Wolfgang-Gaede-Strasse 1, D-76131 Karlsruhe, Germany

<sup>2</sup>Physikalisches Institut, Karlsruhe Institute of Technology, Wolfgang-Gaede-Strasse 1, D-76131 Karlsruhe, Germany

<sup>3</sup>Institute for Quantum Materials and Technologies, Karlsruhe Institute of Technology, D-76344 Eggenstein-Leopoldshafen, Germany

<sup>4</sup>Institute for Theory of Condensed Matter, Karlsruhe Institute of Technology, D-76131 Karlsruhe, Germany



(Received 21 November 2022; revised 23 April 2023; accepted 27 April 2023; published 12 May 2023)

Monolayers of two-dimensional (2D) van der Waals (vdW) materials grown on dielectric oxides exhibit unprecedented physical properties. For example, the superconducting transition temperature of an FeSe monolayer on SrTiO<sub>3</sub> is by far higher than its bulk counterpart. However, how the charge distribution across the interface looks like and how it helps to improve these properties is hitherto unknown. Here, using momentum- and energy-resolved high-resolution electron spectroscopy, we probe the dynamic charge response of the FeSe/SrTiO<sub>3</sub>(001) heterostructures and, thereby, demonstrate the existence of a charge depletion layer at the interface. The presence of this depletion layer, accompanied with a considerably large charge transfer, leads to a renormalization of the SrTiO<sub>3</sub> energy bands and a substantial band bending at the interface. Our discovery paves the way for designing novel 2D superconductors through interface engineering. The phenomenon is expected to occur at the interface of many vdW monolayers and dielectric oxides.

DOI: [10.1103/PhysRevB.107.184508](https://doi.org/10.1103/PhysRevB.107.184508)

## I. INTRODUCTION

The discovery of two-dimensional (2D) van der Waals (vdW) materials has opened up new horizons for novel functional architectures [1–3]. When these materials are grown on a substrate in the form of a monolayer (ML), they may show unexpected electrical, optical, and magnetic properties, which can be precisely controlled by several means, opening up new opportunities for their application in nanoscale devices [4]. The most prominent example of this kind is FeSe ML grown on SrTiO<sub>3</sub>(001) [hereafter STO(001) or STO], with a remarkably high superconducting transition temperature  $T_c$ , the highest among all iron-based superconductors [5–11]. Although the physical mechanism leading to the high-temperature superconductivity (HTSC) in FeSe/STO is not yet fully understood, it is generally believed that superconductivity in this hybrid system is largely enhanced by interfacial effects [12–17]. It has been observed by means of several experimental techniques that FeSe ML is strongly electron doped [8,13,16,18,19–23]. The large carrier density inside FeSe ML has been postulated to be due to the charge transfer from STO into the film [14,19,21–24]. However, the answer to the question of whether these charge carriers originate from the interface or from deeper STO layers has remained elusive. If the charges originate from the STO substrate, this would lead to a charge imbalance in the system, which would then tremendously change the properties of FeSe ML.

Here, by probing the dynamic charge response of the FeSe/STO interface, by means of high-resolution spec-

troscopy of slow electrons we show that the experimentally measured frequency and momentum-resolved dynamic charge response cannot be explained by assuming a simple film/substrate model only. Our detailed analysis unambiguously identifies a charge-free depletion region in the STO substrate at the interface with FeSe ML, accompanied with a considerably large charge transfer from STO into FeSe ML. The presence of the depletion region along with the large interfacial charge transfer leads to a substantial band bending, renormalization of the electronic bands at the interface, and an interfacial electric field. Such an electric field would substantially modify the properties of FeSe ML. In addition to the fact that our findings contribute to the understanding of HTSC in FeSe ML, they would provide guidelines for designing new high-temperature superconductors through interface engineering. Moreover, the formation of a depletion layer at the interface is rather general and is expected to be observed in many combinations of vdW MLs put in contact with dielectric oxides or semiconducting substrates. We will show how such depletion layers can be quantitatively identified by probing the dynamic charge response.

## II. RESULTS

The frequency and momentum-resolved dynamic charge response of the epitaxial FeSe MLs grown on Nb-STO was probed by means of high-resolution electron energy-loss spectroscopy (HREELS) using slow electrons [25]. Figure 1(a) shows the HREEL spectra recorded on the surface of FeSe ML on Nb-STO(001). The spectra were recorded at a temperature of  $T = 15$  K, below  $T_c$  and at two different incident beam energies, namely,  $E_i = 4.07$  eV and  $E_i = 7.23$  eV. The

\*khalil.zakeri@kit.edu

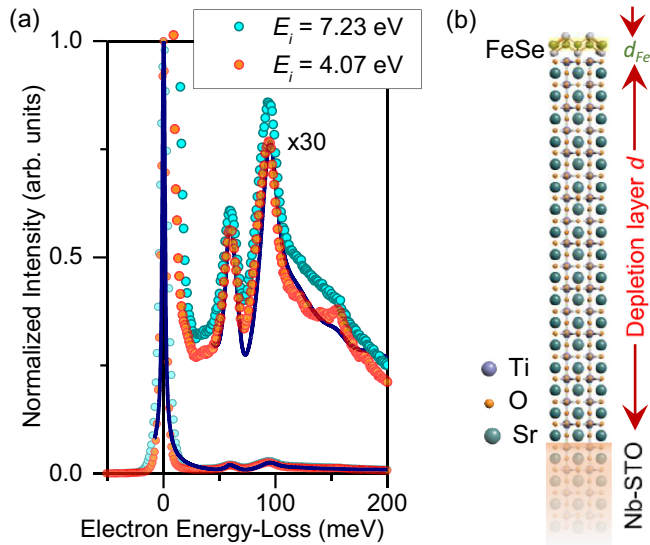


FIG. 1. (a) The experimental spectra recorded at the high symmetry  $\bar{\Gamma}$  point and using two different incident beam energies ( $E_i = 4.07$  eV, orange circles and  $E_i = 7.23$  eV, light-blue circles). The simulated spectrum for  $E_i = 4.07$  eV is represented as the solid line. (b) The geometrical structure used for the simulation. The Fe plane in FeSe ML was placed in a distance  $d_{\text{Fe}} = 0.43$  nm above the STO(001) surface.

spectral function  $S(q_{\parallel}, \omega)$  measured by HREELS directly reflects the dynamical response of the collective charge excitations in the system and is directly proportional to the imaginary part of the dynamic charge susceptibility  $\Im\chi(q, \omega)$  [26,27]. Since the electrons are scattered by the total charge distribution of the sample, the scattering intensity must include information regarding collective ionic excitations, i.e., phonons as well as collective electronic excitations, i.e., plasmons. Moreover, any type of excitation representing a hybrid mode should also be excited within this mechanism. In the measured spectra presented in Fig. 1(a), one observes several interesting features. Besides the elastic peak at the energy loss of  $\hbar\omega = 0$  (zero-loss peak, ZLP) there are small peaks at  $\hbar\omega = 11.8, 20.5, 24.8,$  and  $36.7$  meV. These are the phonon peaks of FeSe ML, which match perfectly to those probed on FeSe(001) single crystals [28–30] and also those reported for the FeSe films on Nb-STO of different thicknesses [31]. The most prominent features are the so-called Fuchs-Kliewer (FK) phonons of STO at  $\hbar\omega = 59.3$  and  $94.5$  meV.

In principle, electrons can also excite multiple quanta (higher-order harmonics) of FK phonons. Hence one should observe these excitations at the multiple frequencies of the principle excitations. The most interesting observation is that unlike the bare STO surfaces [32], in the case of FeSe/STO the higher harmonics of the FK modes are strongly suppressed [33]. We will see that the strong suppression of the higher harmonics of FK modes is due to the presence of the free charge carriers in FeSe ML and in the deeper layers of Nb-STO.

In order to shed light on the origin of the observed phenomenon, the measured HREEL spectra were simulated. The simulation is based on the dipolar scattering theory [25]. Our analysis indicates that considering ML FeSe on a semi-infinite doped STO(001) cannot explain the experimental spectra. The

best model explaining the experimental spectra is considering a system composed of one ML of FeSe on 17 unit cells (UCs) of charge-free insulating STO(001) on top of a semi-infinite Nb-STO(001). The structure is schematically sketched in Fig. 1(b). In this model the Fe plane in FeSe ML is placed in a distance  $d_{\text{Fe}} = 0.43$  nm above the STO(001) surface [34], only in this way both the peak position and amplitude of the excitations associated with the FK modes agree with those measured experimentally, as demonstrated in Fig. 1(a). Similar to the experiment, the higher harmonics of the principle FK modes are strongly suppressed due to the presence of the free carriers in FeSe ML and in the interior part of the substrate, below the depletion region. Spectra calculated for several other configurations and various thicknesses of the depletion layer indicated that the best agreement with the experimental data can be achieved when a depletion layer with a thickness of  $d = 6.5 \pm 1$  nm (or  $17 \pm 3$  UCs) is considered [25].

It has been discussed that the dynamic electric fields associated with FK modes penetrate deeply into the FeSe films [35]. In order to investigate any possible screening of the dynamic electric field of these modes by FeSe ML, we record spectra for various in-plane wave vectors  $q_{\parallel}$ . It was observed that the intensities of the FK modes decreases by three orders of magnitude while increasing  $q_{\parallel}$  from zero to  $0.6 \text{ \AA}^{-1}$  (from the  $\bar{\Gamma}$  towards the  $\bar{X}$  point of the surface Brillouin zone). At the same time the intensity of the ZLP also drops rapidly in a similar manner. Generally, the profile of ZLP as a function of  $q_{\parallel}$  is determined by the presence of defects at the surface. Since in the experiment the incident energy is low (only a few eV), the intensity profile of ZLP shall reflect the surface quality and the surface roughness. In the case of ultrathin films grown on a substrate, such as our samples, the roughness is almost entirely caused by the steps. The strong  $q_{\parallel}$  dependence of the ZLP profile is the signature of low surface roughness and relatively wide terraces. We estimate an average width of at least 100 nm, in agreement with our scanning tunneling microscopy studies [36]. The decrease of the intensity of the FK modes with  $q_{\parallel}$  is almost identical to that of ZLP. This is a strong indication that the observed FK modes at the off-specular geometry are excited via the same mechanism as those at the specular geometry, i.e., the dipolar scattering mechanism. In order to verify this hypothesis, we performed simulations of the HREEL spectra for different geometries as in the experiment. In the experiment the spectra are recorded at the off-specular geometry and both the incident  $\theta_i$  and scattered  $\theta_f$  angles are adjusted to achieve the desired  $q_{\parallel}$ . Since the dipolar scattering theory is only valid in the vicinity of the specular geometry, the condition  $\theta_i = \theta_f$  must be satisfied. Therefore in the simulations only  $\theta_i$  is adjusted to the experimental value. In order to account for the intensity drop of ZLP, the profile of the experimental ZLP is used in the simulation and the results are summarized in Fig. 2. The experimental data are shown in Fig. 2(a), while the results of simulations are presented in Fig. 2(b). The agreement between these two strongly suggests that the FK modes observed at off-specular angles are excited via the dipolar scattering mechanism, as in the specular geometry. The dynamic electric fields generated by fluctuating electric dipoles associated with the FK modes are rather long range. Electrons scattered from the surface would feel these fields far above the surface. This

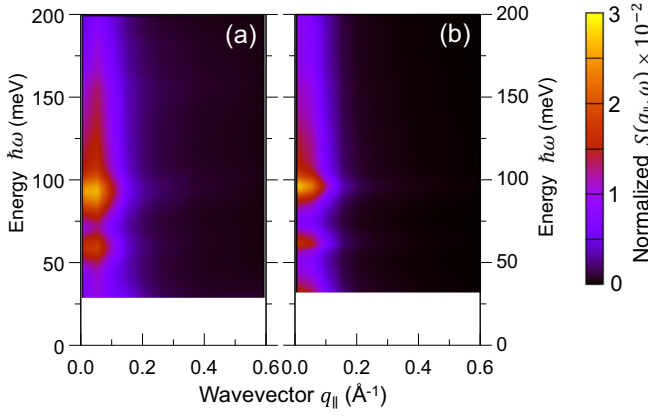


FIG. 2. The experimental (a) and simulated (b) structural factor probed as a function of in-plane momentum and frequency on an FeSe ML grown on Nb-STO(001). The data are recorded at a beam energy of  $E_i = 7.23$  eV. The spectra are normalized to the intensity of the zero-loss peak.

is due to the long-range nature of the Coulomb interaction. The angle under which the electrons are impinged onto the surface and consequently, the parallel momentum of the incoming electron beam are rather unimportant. It seems that the screening effects of ML FeSe on dynamic electric fields is rather small. Such effects are essential to be considered also in other electron spectroscopy experiments, e.g., angle-resolved photoemission spectroscopy (ARPES) [11, 13, 37–42].

Looking at the data presented in Fig. 2 one observes a broad distribution of  $S(q_{\parallel}, \omega)$  in frequency, in particular, for  $\hbar\omega \approx 110$  meV. This is a consequence of the free carriers in FeSe ML as well as in the inner part of Nb-STO. In the spectra recorded at  $E_i = 50$  eV an additional peak has been observed at  $\approx 150$  meV and has been attributed to the response of polaronic plasmons [43]. Our model predicts that this peak originates from the carriers located below the depletion layer, and its presence together with the FK modes is a consequence of the depletion layer [44]. The presence of the charge carriers inside the Nb-STO substrate leads to a broadening and a blueshift of the FK modes [25]. In fact, in such a situation the observed peaks are hybrid modes of both electronic and ionic collective excitations. The dynamic electric fields caused by the fluctuation of FK electrical dipoles are screened by the free carriers. Obviously, at higher  $E_i$  the contribution of the deeper layers is larger in the spectra. One of the consequences of the depletion region at the interface is to enhance the effective dynamic electric field felt by the electrons scattered off (and above) the surface. These electric fields originate mainly from the insulating STO within the depletion region.

### III. DISCUSSION

The observed depletion layer must be tightly connected to the charge transfer from the surface region of Nb-STO into FeSe ML. It has been observed by ARPES as well as tunneling spectroscopy that FeSe ML is heavily electron doped ( $0.12 e^-/\text{Fe atom}$ ) [8, 13, 16, 18–20]. One plausible explanation for such a large charge density is that the carriers are transferred from the top several UCs of Nb-STO into FeSe ML. Doping has been found to greatly enhance  $T_c$  of both

bulk as well as thick FeSe films [18, 45–48]. In order to verify that the charge transfer and the depletion layer are intimately interconnected and to see the consequences of the presence of the depletion layer on the electronic bands, the system was modeled in a similar way as suggested in Refs. [24, 49, 50]. In this model the heavily doped Fe atomic plane in FeSe ML is considered as a charged sheet placed in the distance  $d_{\text{Fe}}$  above the STO(001) [the structure shown in Fig. 1(b)]. The charged sheet generates an electric field and consequently, a displacement vector  $\mathbf{D}$ , which is a function of distance from the charge sheet  $z$ , and extends into the depletion region. After considering the boundary conditions, the generalized displacement vector in the model system sketched in Fig. 1(b) can be written as

$$\mathbf{D}(z) = \begin{cases} \sigma \hat{z} = \mathcal{D} \hat{z} & \text{for } 0 < z \leq d_{\text{Fe}}, \\ \mathcal{D} \left(1 - \frac{z}{\mathfrak{z}}\right) \hat{z} & \text{for } d_{\text{Fe}} \leq z < d, \end{cases} \quad (1)$$

where  $\mathcal{D} = \sigma$  is the surface charge density of the Fe plane and is given by  $\mathcal{D} = 0.24e/a^2$  (here  $a$  represents the in-plane lattice constant of the Fe plane, which is the same as that of FeSe ML).  $d$  is the thickness of the depletion layer after the charge transfer.  $\mathfrak{z}$  is a constant in the units of  $z$ . It is given by the ratio of the surface charge density of the sheet and the volume charge density inside Nb-STO (see below). In this model  $z = 0$  is placed on the Fe plane and  $\hat{z}$  is pointing towards the inner part of Nb-STO(001). At an infinitesimal distance  $\delta$  just above the STO surface, the displacement vector is given by  $\mathbf{D}(z = d_{\text{Fe}} - \delta) = \sigma$ . On the other hand, just below the surface inside STO at  $z = d_{\text{Fe}} + \delta$ ,  $\mathbf{D}$  is given by  $\nabla \cdot \mathbf{D}(z) |_{z=d_{\text{Fe}}+\delta} = -en$ , where  $n$  is the carrier density inside Nb-STO ( $n = 1.18 \times 10^{26} \text{ m}^{-3}$ ). In order to estimate  $\mathfrak{z}$  one may use the boundary conditions. The field continuity at the interface [ $\mathbf{D}(z = d_{\text{Fe}} - \delta) = \mathbf{D}(z = d_{\text{Fe}} + \delta)$ ] implies that  $\mathfrak{z} = \sigma/n \simeq 34$  UCs. The thickness of the depletion layer after the charge transfer shall, however, be smaller than this value. The value found by analyzing the HREEL spectra was  $d \simeq 6.5 \pm 1$  nm ( $17 \pm 3$  UCs).

In order to estimate the band bending above the STO surface and inside the depletion layer the potential profile  $\phi(z)$  should be calculated based on  $\mathbf{D}(z) = -\varepsilon_{\text{STO}}[D(z)]\nabla\phi(z)$ . We note that due to the ferroelectric behavior of STO its dielectric constant  $\varepsilon_{\text{STO}}$  is no longer a constant and depends on  $D$ . Using the function suggested in Refs. [19, 49] for  $\varepsilon(D)$ , the potential was calculated and the results are summarized in Fig. 3. The STO band gap was assumed to be 3.2 eV.

When FeSe ML and Nb-STO are far apart they possess different work functions and their Fermi levels are located at different energies [for an illustration see the sketches in Fig. 3(a)]. Upon attaching these two materials, FeSe ML is negatively charged and a potential will be built up at the interface. Recently, it has been proposed that the Se layer plays an important role in the charge transfer [51]. The profile of the built-in potential near the interface is presented in Fig. 3(a). The magnitude of this potential is large enough to balance the Fermi levels of the two materials and, at the same time, lead to a charge transfer. Such a built-in potential leads to a band bending in the STO in the vicinity of the interface. The profile shown in Fig. 3(b) shows how the valence and conduction band just above the STO surface and also in the depletion

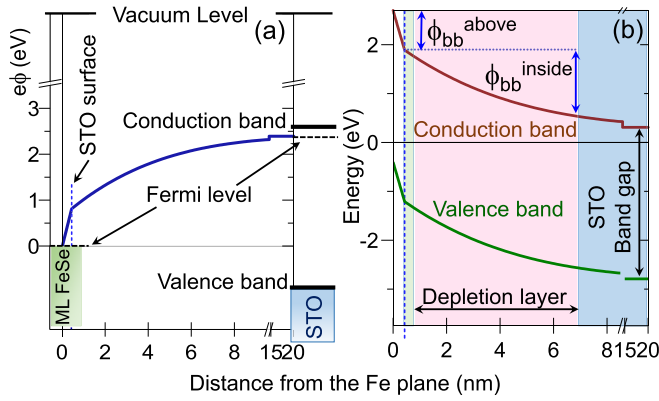


FIG. 3. (a) A schematic representation of the electronic bands of FeSe ML and those of Nd-STO, when they are far apart. The electronic bands of FeSe ML are filled up to the Fermi level, shown by the shaded green area. The filled states of STO are shown by the shaded blue area. The curve represents the calculated potential profile due to the charge transfer as a function of the distance from the Fe plane, when these two are brought in contact. Fermi levels are shown by the dashed horizontal lines. The reference is put on the Fermi level of FeSe ML. (b) The band bending of the STO substrate in the vicinity of the interface, above  $e\phi_{bb}^{\text{above}} = 0.8$  eV and inside  $e\phi_{bb}^{\text{inside}} = 1.3$  eV, the depletion layer.

layer are altered. Our analysis indicates a band bending of the conduction and valence band of about  $e\phi_{bb}^{\text{inside}} = 1.3$  eV inside the depletion region. This is estimated based on the built-in potential profile and represents the potential difference of the STO surface and the edge of the depletion region. The value of  $e\phi_{bb}^{\text{inside}}$  is in agreement with the values of 0.7 eV and 0.4 eV reported for an 8- and a 14-ML-thick film, respectively [14]. In Ref. [19] a band bending in the range of 0.1–0.6 eV has been reported for the FeSe ML, depending on the preparation condition. The presence of the depletion layer at the FeSe/STO interface would also lead to a redistribution of charges at the interface. The strong variation of the potential in the vicinity of the interface just above the STO surface and below the Fe plane is about  $e\phi_{bb}^{\text{above}} = 0.8$  eV. Moreover, the interfacial electric field can induce a Rashba-Dresselhaus type of spin-orbit coupling and lead to interesting spin-dependent effects, as has recently been reported [52].

In the case of bulk FeSe it has been discussed that the Cooper pairing mechanism is mediated by spin fluctuations [53–59]. In the case of FeSe/STO the electronic structure is significantly simpler. The Fermi surface consists of only two electron bands near the zone boundary. The hole pockets are located below the Fermi level by about 80 meV. Hence it is not straightforward to imagine an electronic coupling via the

well-known ( $\pi$ – $\pi$ ) spin fluctuations [60]. However, unconventional pairing states may emerge from other states within the electronic bands [61,62], as has been observed by means of tunneling spectroscopy experiments [36,63]. The spin-orbit coupling induced or boosted by the interfacial electric field can play a decisive role in this scenario [64].

On the other hand, observation of the replica bands in ARPES experiments has been considered as an indication of a phonon-mediated superconductivity in this system [7,11,13,37,39–41]. This suggestion is based on probing the quasiparticle band dispersions, and no solid evidence has been reported by probing the phononic excitations of the system. It has also been suggested that a cooperative effect of several bosonic excitations may be responsible for the high  $T_c$  of this system [16,40,65]. Irrespective of the pairing mechanism responsible for the superconductivity, the observed depletion layer, the large band renormalizations, and the associated interfacial electric field have very important consequences on the properties of FeSe ML [24,38].

#### IV. CONCLUSION

In conclusion, by probing the dynamic charge response of the FeSe superconducting ML on STO, we identified a charge depletion layer at the interface. The formation of the depletion layer explains the long-standing question regarding the origin of the large charge density in FeSe ML when it is grown on STO(001). The existence of the depletion layer has several consequences on the electronic properties of the system. We anticipate that the observed phenomenon is general and exists also at the interface of superconducting monolayers with many other oxide substrates, allowing an interfacial engineering of the superconducting states either by growing ML FeSe on other dielectric surfaces or by growing MLs of other high-temperature superconducting materials on dielectric oxides. Moreover, the observed effect is also of great importance for nonsuperconducting vdW MLs put in contact with oxide or semiconducting substrates. In a similar way, the exotic properties of these vdW MLs can be altered/tuned through interfacing with dielectric oxides.

#### ACKNOWLEDGMENTS

Kh.Z. acknowledges funding from the Deutsche Forschungsgemeinschaft (DFG) through the Heisenberg Programme ZA 902/3-1 and ZA 902/6-1 and the DFG Grant ZA 902/5-1. The research of J.J. and W.W. was supported by DFG through Grant No. Wu 394/12-1. The research of J.S. was supported by DFG via Grant No. SCHM 1031/7-1. F.Y. acknowledges funding from the Alexander von Humboldt Foundation. Kh.Z. thanks the Physikalisches Institut for hosting the group and providing the necessary infrastructure.

- [1] A. K. Geim and I. V. Grigorieva, Van der Waals heterostructures, *Nature (London)* **499**, 419 (2013).
- [2] K. S. Novoselov, A. Mishchenko, A. Carvalho, and A. H. C. Neto, 2D materials and van der Waals heterostructures, *Science* **353**, aac9439 (2016).
- [3] X. Jiang, Q. Liu, J. Xing, N. Liu, Y. Guo, Z. Liu, and J. Zhao, Recent progress on 2D magnets: Fundamental

- mechanism, structural design and modification, *Appl. Phys. Rev.* **8**, 031305 (2021).
- [4] Y. Liu, N. O. Weiss, X. Duan, H.-C. Cheng, Y. Huang, and X. Duan, Van der Waals heterostructures and devices, *Nat. Rev. Mater.* **1**, 16042 (2016).
- [5] Q.-Y. Wang, Z. Li, W.-H. Zhang, Z.-C. Zhang, J.-S. Zhang, W. Li, H. Ding, Y.-B. Ou, P. Deng, K. Chang, J. Wen, C.-L. Song,

- K. He, J.-F. Jia, S.-H. Ji, Y.-Y. Wang, L.-L. Wang, X. Chen, X.-C. Ma, and Q.-K. Xue, Interface-induced high-temperature superconductivity in single unit-cell FeSe films on SrTiO<sub>3</sub>, *Chin. Phys. Lett.* **29**, 037402 (2012).
- [6] D. Liu, W. Zhang, D. Mou, J. He, Y.-B. Ou, Q.-Y. Wang, Z. Li, L. Wang, L. Zhao, S. He, Y. Peng, X. Liu, C. Chen, L. Yu, G. Liu, X. Dong, J. Zhang, C. Chen, Z. Xu, J. Hu *et al.*, Electronic origin of high-temperature superconductivity in single-layer FeSe superconductor, *Nat. Commun.* **3**, 931 (2012).
- [7] S. Tan, Y. Zhang, M. Xia, Z. Ye, F. Chen, X. Xie, R. Peng, D. Xu, Q. Fan, H. Xu, J. Jiang, T. Zhang, X. Lai, T. Xiang, J. Hu, B. Xie, and D. Feng, Interface-induced superconductivity and strain-dependent spin density waves in FeSe/SrTiO<sub>3</sub> thin films, *Nat. Mater.* **12**, 634 (2013).
- [8] S. He, J. He, W. Zhang, L. Zhao, D. Liu, X. Liu, D. Mou, Y.-B. Ou, Q.-Y. Wang, Z. Li, L. Wang, Y. Peng, Y. Liu, C. Chen, L. Yu, G. Liu, X. Dong, J. Zhang, C. Chen, Z. Xu *et al.*, Phase diagram and electronic indication of high-temperature superconductivity at 65 K in single-layer FeSe films, *Nat. Mater.* **12**, 605 (2013).
- [9] I. Bozovic and C. Ahn, A new frontier for superconductivity, *Nat. Phys.* **10**, 892 (2014).
- [10] J.-F. Ge, Z.-L. Liu, C. Liu, C.-L. Gao, D. Qian, Q.-K. Xue, Y. Liu, and J.-F. Jia, Superconductivity above 100 K in single-layer FeSe films on doped SrTiO<sub>3</sub>, *Nat. Mater.* **14**, 285 (2015).
- [11] J. J. Lee, F. T. Schmitt, R. G. Moore, S. Johnston, Y.-T. Cui, W. Li, M. Yi, Z. K. Liu, M. Hashimoto, Y. Zhang, D. H. Lu, T. P. Devereaux, D.-H. Lee, and Z.-X. Shen, Interfacial mode coupling as the origin of the enhancement of T<sub>c</sub> in FeSe films on SrTiO<sub>3</sub>, *Nature (London)* **515**, 245 (2014).
- [12] R. Peng, H. C. Xu, S. Y. Tan, H. Y. Cao, M. Xia, X. P. Shen, Z. C. Huang, C. Wen, Q. Song, T. Zhang, B. P. Xie, X. G. Gong, and D. L. Feng, Tuning the band structure and superconductivity in single-layer FeSe by interface engineering, *Nat. Commun.* **5**, 5044 (2014).
- [13] C. Zhang, Z. Liu, Z. Chen, Y. Xie, R. He, S. Tang, J. He, W. Li, T. Jia, S. N. Rebec, E. Y. Ma, H. Yan, M. Hashimoto, D. Lu, S.-K. Mo, Y. Hikita, R. G. Moore, H. Y. Hwang, D. Lee, and Z. Shen, Ubiquitous strong electron-phonon coupling at the interface of FeSe/SrTiO<sub>3</sub>, *Nat. Commun.* **8**, 14468 (2017).
- [14] W. Zhao, M. Li, C.-Z. Chang, J. Jiang, L. Wu, C. Liu, J. S. Moodera, Y. Zhu, and M. H. W. Chan, Direct imaging of electron transfer and its influence on superconducting pairing at FeSe/SrTiO<sub>3</sub> interface, *Sci. Adv.* **4**, eaao2682 (2018).
- [15] G. Zhou, Q. Zhang, F. Zheng, D. Zhang, C. Liu, X. Wang, C.-L. Song, K. He, X.-C. Ma, L. Gu, P. Zhang, L. Wang, and Q.-K. Xue, Interface enhanced superconductivity in monolayer FeSe films on MgO(001): Charge transfer with atomic substitution, *Sci. Bull.* **63**, 747 (2018).
- [16] Q. Song, T. L. Yu, X. Lou, B. P. Xie, H. C. Xu, C. H. P. Wen, Q. Yao, S. Y. Zhang, X. T. Zhu, J. D. Guo, R. Peng, and D. L. Feng, Evidence of cooperative effect on the enhanced superconducting transition temperature at the FeSe/SrTiO<sub>3</sub> interface, *Nat. Commun.* **10**, 758 (2019).
- [17] X. Xu, S. Zhang, X. Zhu, and J. Guo, Superconductivity enhancement in FeSe/SrTiO<sub>3</sub>: A review from the perspective of electron-phonon coupling, *J. Phys.: Condens. Matter* **32**, 343003 (2020).
- [18] J. J. Seo, B. Y. Kim, B. S. Kim, J. K. Jeong, J. M. Ok, J. S. Kim, J. D. Denlinger, S. K. Mo, C. Kim, and Y. K. Kim, Superconductivity below 20K in heavily electron-doped surface layer of FeSe bulk crystal, *Nat. Commun.* **7**, 11116 (2016).
- [19] H. Zhang, D. Zhang, X. Lu, C. Liu, G. Zhou, X. Ma, L. Wang, P. Jiang, Q.-K. Xue, and X. Bao, Origin of charge transfer and enhanced electron-phonon coupling in single unit-cell FeSe films on SrTiO<sub>3</sub>, *Nat. Commun.* **8**, 214 (2017).
- [20] X. Shi, Z.-Q. Han, X.-L. Peng, P. Richard, T. Qian, X.-X. Wu, M.-W. Qiu, S. C. Wang, J. P. Hu, Y.-J. Sun, and H. Ding, Enhanced superconductivity accompanying a Lifshitz transition in electron-doped FeSe monolayer, *Nat. Commun.* **8**, 14988 (2017).
- [21] S. N. Rebec, T. Jia, C. Zhang, M. Hashimoto, D.-H. Lu, R. G. Moore, and Z.-X. Shen, Coexistence of Replica Bands and Superconductivity in FeSe Monolayer Films, *Phys. Rev. Lett.* **118**, 067002 (2017).
- [22] Y. Song, Z. Chen, Q. Zhang, H. Xu, X. Lou, X. Chen, X. Xu, X. Zhu, R. Tao, T. Yu, H. Ru, Y. Wang, T. Zhang, J. Guo, L. Gu, Y. Xie, R. Peng, and D. Feng, High temperature superconductivity at FeSe/LaFeO<sub>3</sub> interface, *Nat. Commun.* **12**, 5926 (2021).
- [23] K. Ide, T. Tanaka, A. Pedersen, S. Ichinokura, and T. Hirahara, Temperature dependence of the superconducting gap of single-layer FeSe/STO: Direct comparison between transport and spectroscopic measurements, *Phys. Rev. Mater.* **6**, 124801 (2022).
- [24] Y. Zhou and A. J. Millis, Charge transfer and electron-phonon coupling in monolayer FeSe on Nb-doped SrTiO<sub>3</sub>, *Phys. Rev. B* **93**, 224506 (2016).
- [25] See Supplemental Material at <http://link.aps.org/supplemental/10.1103/PhysRevB.107.184508> for detailed information on our sample preparation, experimental setup for electron spectroscopy, the method of probing the dynamic charge response and the numerical method for the simulations of the spectra. Supplemental Material also provides additional data, supporting our statement in the manuscript. We provide experimental HREELS data recorded on a clean STO surface along with the corresponding simulation. Moreover, we show spectra simulated for several different cases and with various thicknesses of the depletion layer. The Supplemental Material contains Refs. [6,8,10–14,16–21,23,24,29,32,36,38,43,66–86].
- [26] S. Vig, A. Kogar, M. Mitrano, A. Husain, L. Venema, M. Rak, V. Mishra, P. Johnson, G. Gu, E. Fradkin, M. Norman, and P. Abbamonte, Measurement of the dynamic charge response of materials using low-energy, momentum-resolved electron energy-loss spectroscopy (M-EELS), *SciPost Phys.* **3**, 026 (2017).
- [27] A. A. Husain, M. Mitrano, M. S. Rak, S. Rubeck, B. Uchoa, K. March, C. Dwyer, J. Schneeloch, R. Zhong, G. D. Gu, and P. Abbamonte, Crossover of Charge Fluctuations Across the Strange Metal Phase Diagram, *Phys. Rev. X* **9**, 041062 (2019).
- [28] V. Gnezdilov, Y. G. Pashkevich, P. Lemmens, D. Wulferding, T. Shevtsova, A. Gusev, D. Chareev, and A. Vasiliev, Interplay between lattice and spin states degree of freedom in the fese superconductor: Dynamic spin state instabilities, *Phys. Rev. B* **87**, 144508 (2013).
- [29] K. Zakeri, T. Engelhardt, T. Wolf, and M. Le Tacon, Phonon dispersion relation of single-crystalline  $\beta$ -FeSe, *Phys. Rev. B* **96**, 094531 (2017).

- [30] K. Zakeri, T. Engelhardt, M. L. Tacon, and T. Wolf, Phonon spectrum of single-crystalline FeSe probed by high-resolution electron energy-loss spectroscopy, *Physica C* **549**, 18 (2018).
- [31] S. Zhang, J. Guan, Y. Wang, T. Berlijn, S. Johnston, X. Jia, B. Liu, Q. Zhu, Q. An, S. Xue, Y. Cao, F. Yang, W. Wang, J. Zhang, E. W. Plummer, X. Zhu, and J. Guo, Lattice dynamics of ultrathin FeSe films on SrTiO<sub>3</sub>, *Phys. Rev. B* **97**, 035408 (2018).
- [32] T. Conard, L. Philippe, P. Thiry, P. Lambin, and R. Caudano, Electron energy-loss spectroscopy and dynamics of SrTiO<sub>3</sub>(100), *Surf. Sci. Lett.* **287-288**, A390 (1993).
- [33] Note that within the dipolar scattering mechanism for a semi-infinite substrate, the intensities of dipolar losses normalized to the elastic peak intensity scale in a  $1/\sqrt{E_i}$  manner, where  $E_i$  is the energy of the incident electron beam. This means that the lower the incident energy, the larger the amplitude of FK modes. The intensities of the higher-order harmonics of FK modes obey a Poisson distribution [70]. Hence, in the spectra recorded using such low incident energies, one shall clearly observe both the FK modes and their higher-order harmonics, if they are present in the system.
- [34] R. Peng, K. Zou, M. G. Han, S. D. Albright, H. Hong, C. Lau, H. C. Xu, Y. Zhu, F. J. Walker, and C. H. Ahn, Picoscale structural insight into superconductivity of monolayer FeSe/SrTiO<sub>3</sub>, *Sci. Adv.* **6**, eaay4517 (2020).
- [35] S. Zhang, J. Guan, X. Jia, B. Liu, W. Wang, F. Li, L. Wang, X. Ma, Q. Xue, J. Zhang, E. W. Plummer, X. Zhu, and J. Guo, Role of SrTiO<sub>3</sub> phonon penetrating into thin FeSe films in the enhancement of superconductivity, *Phys. Rev. B* **94**, 081116(R) (2016).
- [36] J. Jandke, F. Yang, P. Hlobil, T. Engelhardt, D. Rau, K. Zakeri, C. Gao, J. Schmalian, and W. Wulfhekkel, Unconventional pairing in single FeSe layers, *Phys. Rev. B* **100**, 020503(R) (2019).
- [37] Y. Wang, A. Linscheid, T. Berlijn, and S. Johnston, *Ab initio* study of cross-interface electron-phonon couplings in FeSe thin films on SrTiO<sub>3</sub>, *Phys. Rev. B* **93**, 134513 (2016).
- [38] Y. Zhou and A. J. Millis, Dipolar phonons and electronic screening in monolayer FeSe on SrTiO<sub>3</sub>, *Phys. Rev. B* **96**, 054516 (2017).
- [39] B. D. Faeth, S. Xie, S. Yang, J. K. Kawasaki, J. N. Nelson, S. Zhang, C. Parzyck, P. Mishra, C. Li, C. Jozwiak, A. Bostwick, E. Rotenberg, D. G. Schlom, and K. M. Shen, Interfacial Electron-Phonon Coupling Constants Extracted from Intrinsic Replica Bands in Monolayer FeSe/SrTiO<sub>3</sub>, *Phys. Rev. Lett.* **127**, 016803 (2021).
- [40] L. Rademaker, G. Alvarez-Suchini, K. Nakatsukasa, Y. Wang, and S. Johnston, Enhanced superconductivity in FeSe/SrTiO<sub>3</sub> from the combination of forward scattering phonons and spin fluctuations, *Phys. Rev. B* **103**, 144504 (2021).
- [41] C. Liu, R. P. Day, F. Li, R. L. Roemer, S. Zhdanovich, S. Gorovikov, T. M. Pedersen, J. Jiang, S. Lee, M. Schneider, D. Wong, P. Dosanjh, F. J. Walker, C. H. Ahn, G. Levy, A. Damascelli, G. A. Sawatzky, and K. Zou, High-order replica bands in monolayer FeSe/SrTiO<sub>3</sub> revealed by polarization-dependent photoemission spectroscopy, *Nat. Commun.* **12**, 4573 (2021).
- [42] F. Li and G. A. Sawatzky, Electron Phonon Coupling Versus Photoelectron Energy Loss at the Origin of Replica Bands in Photoemission of FeSe on SrTiO<sub>3</sub>, *Phys. Rev. Lett.* **120**, 237001 (2018).
- [43] S. Zhang, T. Wei, J. Guan, Q. Zhu, W. Qin, W. Wang, J. Zhang, E. W. Plummer, X. Zhu, Z. Zhang, and J. Guo, Enhanced Superconducting State in FeSe/SrTiO<sub>3</sub> by a Dynamic Interfacial Polaron Mechanism, *Phys. Rev. Lett.* **122**, 066802 (2019).
- [44] This fact that in HREELS experiments excitations associated with the deeper part of the samples are better observed at higher incident energies is well known [70,71,87]. The reason is that in the standard description of HREELS collective charge excitations exhibit amplitudes which decay exponentially from the surface into the bulk with a decay length of  $1/q_{\parallel}$ . The parallel component of the wave vector  $q_{\parallel}$  is proportional to  $k_i/E_i$ , where  $k_i$  and  $E_i$  represent the momentum and the energy of the incident electron, respectively. Hence, a larger incident energy decreases  $q_{\parallel}$  and therefore increases the “penetration depth” of the excitations. This means that the apparent probing depth of HREELS increases with  $E_i$ .
- [45] T. Qian, X.-P. Wang, W.-C. Jin, P. Zhang, P. Richard, G. Xu, X. Dai, Z. Fang, J.-G. Guo, X.-L. Chen, and H. Ding, Absence of a Holelike Fermi Surface for the Iron-Based KFeSe Superconductor Revealed by Angle-Resolved Photoemission Spectroscopy, *Phys. Rev. Lett.* **106**, 187001 (2011).
- [46] Y. Zhang, L. X. Yang, M. Xu, Z. R. Ye, F. Chen, C. He, H. C. Xu, J. Jiang, B. P. Xie, J. J. Ying, X. F. Wang, X. H. Chen, J. P. Hu, M. Matsunami, S. Kimura, and D. L. Feng, Nodeless superconducting gap in A<sub>x</sub>Fe<sub>2</sub>Se<sub>2</sub> (A=K,Cs) revealed by angle-resolved photoemission spectroscopy, *Nat. Mater.* **10**, 273 (2011).
- [47] Y. Miyata, K. Nakayama, K. Sugawara, T. Sato, and T. Takahashi, High-temperature superconductivity in potassium-coated multilayer FeSe thin films, *Nat. Mater.* **14**, 775 (2015).
- [48] B. Lei, J. H. Cui, Z. J. Xiang, C. Shang, N. Z. Wang, G. J. Ye, X. G. Luo, T. Wu, Z. Sun, and X. H. Chen, Evolution of High-Temperature Superconductivity from a Low-T<sub>c</sub> Phase Tuned by Carrier Concentration in FeSe Thin Flakes, *Phys. Rev. Lett.* **116**, 077002 (2016).
- [49] M. Stengel, First-Principles Modeling of Electrostatically Doped Perovskite Systems, *Phys. Rev. Lett.* **106**, 136803 (2011).
- [50] K. V. Reich, M. Schechter, and B. I. Shklovskii, Accumulation, inversion, and depletion layers in SrTiO<sub>3</sub>, *Phys. Rev. B* **91**, 115303 (2015).
- [51] F. Li, I. Elfimov, and G. A. Sawatzky, Modulation doping of the FeSe monolayer on SrTiO<sub>3</sub>, *Phys. Rev. B* **105**, 214518 (2022).
- [52] K. Zakeri, D. Rau, J. Jandke, F. Yang, W. Wulfhekkel, and C. Berthod, Direct probing of a large spin-orbit coupling in the FeSe superconducting monolayer on STO, *ACS Nano* (2023), doi: 10.1021/acsnano.3c02876.
- [53] Q. Wang, Y. Shen, B. Pan, Y. Hao, M. Ma, F. Zhou, P. Steffens, K. Schmalzl, T. Forrest, M. Abdel-Hafiez *et al.*, Strong interplay between stripe spin fluctuations, nematicity and superconductivity in FeSe, *Nat. Mater.* **15**, 159 (2016).
- [54] T. Chen, Y. Chen, A. Kreisel, X. Lu, A. Schneidewind, Y. Qiu, J. T. Park, T. G. Perring, J. R. Stewart, H. Cao, R. Zhang, Y. Li, Y. Rong, Y. Wei, B. M. Andersen, P. J. Hirschfeld, C. Broholm, and P. Dai, Anisotropic spin fluctuations in detwinned FeSe, *Nat. Mater.* **18**, 709 (2019).
- [55] D. Phelan, J. N. Millican, E. L. Thomas, J. B. Leão, Y. Qiu, and R. Paul, Neutron scattering measurements of the phonon density of states of FeSe<sub>1-x</sub> superconductors, *Phys. Rev. B* **79**, 014519 (2009).

- [56] Q.-Q. Ye, K. Liu, and Z.-Y. Lu, Influence of spin-phonon coupling on antiferromagnetic spin fluctuations in FeSe under pressure: First-principles calculations with van der Waals corrections, *Phys. Rev. B* **88**, 205130 (2013).
- [57] I. I. Mazin, Superconductivity: The FeSe riddle, *Nat. Mater.* **14**, 755 (2015).
- [58] F. Schrodi, A. Aperis, and P. M. Oppeneer, Eliashberg theory for spin fluctuation mediated superconductivity: Application to bulk and monolayer FeSe, *Phys. Rev. B* **102**, 014502 (2020).
- [59] S. Acharya, D. Pashov, F. Jamet, and M. van Schilfgaarde, Electronic origin of Tc in bulk and monolayer FeSe, *Symmetry* **13**, 169 (2021).
- [60] J. Pellicciari, S. Karakuzu, Q. Song, R. Arpaia, A. Nag, M. Rossi, J. Li, T. Yu, X. Chen, R. Peng, M. García-Fernández, A. C. Walters, Q. Wang, J. Zhao, G. Ghiringhelli, D. Feng, T. A. Maier, K.-J. Zhou, S. Johnston, and R. Comin, Evolution of spin excitations from bulk to monolayer FeSe, *Nat. Commun.* **12**, 3122 (2021).
- [61] S. Graser, T. A. Maier, P. J. Hirschfeld, and D. J. Scalapino, Near-degeneracy of several pairing channels in multiorbital models for the Fe pnictides, *New J. Phys.* **11**, 025016 (2009).
- [62] A. Linscheid, S. Maiti, Y. Wang, S. Johnston, and P. J. Hirschfeld, High  $T_C$  via Spin Fluctuations from Incipient Bands: Application to Monolayers and Intercalates of FeSe, *Phys. Rev. Lett.* **117**, 077003 (2016).
- [63] C. Liu, Z. Wang, S. Ye, C. Chen, Y. Liu, Q. Wang, Q.-H. Wang, and J. Wang, Detection of bosonic mode as a signature of magnetic excitation in one-unit-cell FeSe on SrTiO<sub>3</sub>, *Nano Lett.* **19**, 3464 (2019).
- [64] S. V. Borisenko, D. V. Evtushinsky, Z.-H. Liu, I. Morozov, R. Kappenberger, S. Wurmehl, B. Büchner, A. N. Yaresko, T. K. Kim, M. Hoesch, T. Wolf, and N. D. Zhigadlo, Direct observation of spin-orbit coupling in iron-based superconductors, *Nat. Phys.* **12**, 311 (2016).
- [65] F. Schrodi, A. Aperis, and P. M. Oppeneer, Multichannel superconductivity of monolayer FeSe on SrTiO<sub>3</sub>: Interplay of spin fluctuations and electron-phonon interaction, *Phys. Rev. B* **102**, 180501(R) (2020).
- [66] Z. Li, J.-P. Peng, H.-M. Zhang, W.-H. Zhang, H. Ding, P. Deng, K. Chang, C.-L. Song, S.-H. Ji, L. Wang, K. He, X. Chen, Q.-K. Xue, and X.-C. Ma, Molecular beam epitaxy growth and post-growth annealing of FeSe films on SrTiO<sub>3</sub>: A scanning tunneling microscopy study, *J. Phys.: Condens. Matter* **26**, 265002 (2014).
- [67] H. Ibach, D. Bruchmann, R. Vollmer, M. Etzkorn, P. S. A. Kumar, and J. Kirschner, A novel spectrometer for spin-polarized electron energy-loss spectroscopy, *Rev. Sci. Instrum.* **74**, 4089 (2003).
- [68] R. Vollmer, M. Etzkorn, P. S. A. Kumar, H. Ibach, and J. Kirschner, Spin-Polarized Electron Energy Loss Spectroscopy of High Energy, Large Wave Vector Spin Waves in Ultrathin fcc Co Films on Cu(001), *Phys. Rev. Lett.* **91**, 147201 (2003).
- [69] K. Zakeri, Elementary spin excitations in ultrathin itinerant magnets, *Phys. Rep.* **545**, 47 (2014).
- [70] H. Ibach and D. Mills, *Electron Energy Loss Spectroscopy and Surface Vibrations* (Academic, New York, 1982), pp. 105–120.
- [71] A. Ritz and H. Lüth, Experimental Evidence for Surface Quenching of the Surface Plasmon on InSb(110), *Phys. Rev. Lett.* **52**, 1242 (1984).
- [72] W. L. Schaich, Surface Quenching or Surface Depletion? *Phys. Rev. Lett.* **53**, 2059 (1984).
- [73] H. Lüth, Electron energy loss spectroscopy applied to semiconductor space charge layers, *Vacuum* **38**, 223 (1988).
- [74] K. Zakeri, J. Wettstein, and C. Sürgers, Generation of spin-polarized hot electrons at topological insulators surfaces by scattering from collective charge excitations, *Commun. Phys.* **4**, 225 (2021).
- [75] M. Šunjić and A. A. Lucas, Multiple plasmon effects in the energy-loss spectra of electrons in thin films, *Phys. Rev. B* **3**, 719 (1971).
- [76] A. A. Lucas and M. Šunjić, Fast-electron spectroscopy of collective excitations in solids, *Prog. Surf. Sci.* **2**, 75 (1972).
- [77] P. Lambin, J.-P. Vigneron, and A. Lucas, Computation of the surface electron-energy-loss spectrum in specular geometry for an arbitrary plane-stratified medium, *Comput. Phys. Commun.* **60**, 351 (1990).
- [78] R. Lazzari, J. Li, and J. Jupille, Dielectric study of the interplay between charge carriers and electron energy losses in reduced titanium dioxide, *Phys. Rev. B* **98**, 075432 (2018).
- [79] R. H. Yuan, T. Dong, Y. J. Song, P. Zheng, G. F. Chen, J. P. Hu, J. Q. Li, and N. L. Wang, Nanoscale phase separation of antiferromagnetic order and superconductivity in K<sub>0.75</sub>Fe<sub>1.75</sub>Se<sub>2</sub>, *Sci. Rep.* **2**, 221 (2012).
- [80] F. Gervais, J.-L. Servoin, A. Baratoff, J. G. Bednorz, and G. Binnig, Temperature dependence of plasmons in Nb-doped SrTiO<sub>3</sub>, *Phys. Rev. B* **47**, 8187 (1993).
- [81] J. Galzerani and R. Katiyar, The infrared reflectivity in SrTiO<sub>3</sub> and the antidistortive transition, *Solid State Commun.* **41**, 515 (1982).
- [82] D. M. Eagles, M. Georgiev, and P. C. Petrova, Explanation for the temperature dependence of plasma frequencies in SrTiO<sub>3</sub> using mixed-polaron theory, *Phys. Rev. B* **54**, 22 (1996).
- [83] C. Collignon, P. Bourges, B. Fauqué, and K. Behnia, Heavy Nondegenerate Electrons in Doped Strontium Titanate, *Phys. Rev. X* **10**, 031025 (2020).
- [84] C. Chen, J. Avila, E. Frantzeskakis, A. Levy, and M. C. Asensio, Observation of a two-dimensional liquid of Fröhlich polarons at the bare SrTiO<sub>3</sub> surface, *Nat. Commun.* **6**, 8585 (2015).
- [85] S. N. Rebec, T. Jia, H. M. Sohail, M. Hashimoto, D. Lu, Z.-X. Shen, and R. G. Moore, Dichotomy of the photo-induced 2-dimensional electron gas on SrTiO<sub>3</sub> surface terminations, *Proc. Natl. Acad. Sci. USA* **116**, 16687 (2019).
- [86] E. B. Guedes, S. Muff, W. H. Brito, M. Caputo, H. Li, N. C. Plumb, J. H. Dil, and M. Radović, Universal structural influence on the 2D electron gas at SrTiO<sub>3</sub> surfaces, *Adv. Sci.* **8**, 2100602 (2021).
- [87] K. Zakeri and C. Berthod, Theory of spin-polarized high-resolution electron energy loss spectroscopy from nonmagnetic surfaces with a large spin-orbit coupling, *Phys. Rev. B* **106**, 235117 (2022).